þÿ T h e f r e q u e n c y o f i s o m e r i z a t i o n - l i k e d a r k e v e n t and porphyropsin rods of the bullfrog retina

Donner, K.

Blackwell
1990

Journal of Physiology. 1990. 428: 673-692

http://hdl.handle.net/1975/962

Journal of Physiology (1990), **428**, *pp.* 673–692
With 7 figures
Printed in Great Britain

THE FREQUENCY OF ISOMERIZATION-LIKE 'DARK' EVENTS IN RHODOPSIN AND PORPHYROPSIN RODS OF THE BULL-FROG RETINA

BY K. DONNER*, M. L. FIRSOV AND V. I. GOVARDOVSKII

*From the Sechenov Institute of Evolutionary Physiology and Biochemistry, USSR Academy of Sciences, Leningrad, USSR and *Department of Zoology, University of Helsinki, SF-00100 Helsinki, Finland*

(*Received 6 December 1989*)

SUMMARY

1. The dark current and responses to dim flashes were recorded with the suction pipette technique from single rods in pieces of bull-frog retina taken from either the dorsal porphyropsin or the ventral rhodopsin field.

2. The composition of visual pigment in the rods was determined by microspectrophotometry. Rods from the dorsal pieces contained 70–88% porphyropsin$_{523}$ mixed with rhodopsin$_{502}$. The ventral rods contained almost pure rhodopsin, any possible admixture of porphyropsin being below the level of detectability (less than 5%).

3. In most cells, the responses to dim flashes were well fitted by a four-stage linear filter model, with no systematic differences in the response kinetics of porphyropsin and rhodopsin rods. The amplitude of saturated responses varied between 8 and 55 pA and that of responses to single isomerizations between 0·4 and 3·5 pA.

4. In porphyropsin rods, discrete events similar to the response to one photoisomerization were clearly seen in complete darkness. The dark current amplitude histogram was fitted by a convolution of the probability densities for the Gaussian continuous noise component and the averaged dim-flash response waveform. This allows estimation of the frequency and amplitude of discrete events and the standard deviation of the continuous component. The mean frequency of discrete dark events thus obtained from six porphyropsin cells was 0·057 rod^{-1} s^{-1} at 18 °C.

5. In rhodopsin rods, the dark current amplitude histogram appeared completely symmetrical, indicating that the frequency of discrete events must be lower than 0·005 rod^{-1} s^{-1} (except in one rod where it was 0·006 events rod^{-1} s^{-1}). Per molecule of rhodopsin, the events are then at least 5 times rarer than reported for toad rhodopsin rods at the same temperature.

6. The low rate of isomerization-like 'dark' events in bull-frog rhodopsin rods shows, firstly, that results cannot be generalized across species even for rhodopsins which appear spectrally identical. Secondly, it suggests that these events need not (in

Reprint requests to: Dr Kristian Donner, Department of Zoology, University of Helsinki, Arkadiankatu 7, SF-00100 Helsinki, Finland.

MS 8125

an evolutionary sense) constitute an irreducible noise factor which must set the ultimate limit to the sensitivity of dark-adapted vision.

7. The difference between porphyropsin and rhodopsin rods shows that, given (presumably) the same opsin, the pigment utilizing retinal$_2$ and absorbing maximally at longer wavelengths produces more noise. The signal/noise ratio attained in the photoreceptor may be an important factor in the natural selection of visual pigments.

INTRODUCTION

The idea that the sensitivity of dark-adapted vision is ultimately limited by an intrinsic noise due to thermal excitation of the visual pigment has its roots nearly half a century back in time (Autrum, 1943; Barlow, 1956; Ashmore & Falk, 1977). It received direct support when Baylor, Matthews & Yau (1980) reported the occurrence, in the dark current of single toad rods, of discrete events which are indistinguishable from the response to a single photoisomerization. According to present knowledge on transduction in vertebrate rods, the most likely source of such events is the thermal activation of rhodopsin. Subsequently, it has been shown that the dark-adapted sensitivity of many ganglion cells in the toad retina, as well as that of the visually guided prey catching of the toad, is limited by a noise which could well be due mainly to these randomly occurring events (Copenhagen, Donner & Reuter, 1987; Aho, Donner, Hydén, Larsen & Reuter, 1988).

As first noted by Barlow (1957; cf. also Stiles, 1948; de Vries, 1948), simple physical considerations predict that the rate of thermal isomerization of a visual pigment should strongly depend on its wavelength of maximum absorption (λ_{max}). The more red-sensitive the pigment, the lower is the energy barrier for its excitation, and the higher is the probability that the barrier may be overcome by thermal energy alone. This dependence of 'dark' noise on λ_{max} would strongly influence the performance of visual systems using different pigments, favouring the use of short-wavelength pigments for vision in dim light. Barlow proposed that this could be the main reason for the Purkinje shift.

Presently available experimental evidence gives a somewhat contradictory picture. In the toad, the rate of discrete 'dark' events per pigment molecule obtained in the 433 nm green rods (Matthews, 1984) is higher than in the 502 nm red rods (Baylor *et al.* 1980). (The structural difference between the two pigments lies in the protein part.) On the other hand, the rates per molecule in porphyropsin rods of two sturgeon species (λ_{max} = 538 and 549 nm; Firsov & Govardovskii, 1990) have been found to be in qualitative agreement with Barlow's idea: the estimated rate was higher for the 549 than the 538 nm pigment, and the rates of both were one order of magnitude higher than that of toad or monkey rhodopsin (Baylor *et al.* 1980; Baylor, Nunn & Schnapf, 1984). However, considerable interspecies and other differences make the interpretation of these data somewhat problematic.

The bull-frog retina offers the interesting possibility of comparing the dark noise of rods that differ in λ_{max} and the chromophoric group of their visual pigments, but appear to be identical in other respects (Reuter, White & Wald, 1971). The rods in the dorsalmost part of the retina contain predominantly porphyropsin ($\lambda_{max} \approx 523$ nm) and those in the ventral part rhodopsin ($\lambda_{max} \approx 502$ nm). Yet, there

is no basic division into two different classes of rods, because one and the same rod can contain varying proportions of the two pigments depending on the light régime, temperature and other factors (Reuter *et al.* 1971; Tsin & Beatty, 1980; Makino, Kuzuo & Suzuki, 1983).

In the experiments reported here, we determined the frequencies of isomerization-like dark events in porphyropsin-dominated rods and in rhodopsin rods of the bull-frog retina. We find that such events, per molecule of visual pigment, are at least 8 times more frequent in the former than in the latter. The difference is so large that the dependence of noise on λ_{max} (and/or chromophoric group) could well be a major factor in the natural selection of visual pigments. On the other hand, the low rate of dark events we find in the rhodopsin rods of the bull frog compared with values previously reported from rhodopsin rods of toad and monkey (Baylor *et al.* 1980, 1984) casts doubt on the idea that this type of noise constitutes an inexorable limitation to dark-adapted sensitivity.

METHODS

Biological material and preparation

Medium-sized bull-frogs (*Rana catesbeiana*) were procured from KONS Scientific Co., Inc. (Germantown, WI 53022, USA) and kept on a 12 h:12 h light–dark cycle at 15 °C in basins with a white floor, the purpose being to favour the development of the dorsal porphyropsin field (see Tsin & Beatty, 1980). The frogs were used between 1 and 3 months from delivery and were not fed during that time. The night before an experiment, the frog was kept in darkness at room temperature. It was killed and double-pithed and the eyes were enucleated under dim red light. The anterior portion was removed and a small segment of the eyecup was excised from the desired region (dorsal or ventral). The segment was transferred to a Petri dish containing Ringer solution (composition (mM): NaCl, 90; KCl, 2·5; $MgSO_4$, 1·0; $CaCl_2$, 1·0; $NaHCO_3$, 5·0; glucose, 10; HEPES, 10; pH 7·5–7·7) in which the retina was isolated. (A lower Ca^{2+} concentration, 0·5 mM, was used in a few experiments where we attempted to increase the response amplitude of the rods. The practice was abandoned as it appeared to give no advantage in signal/noise, but the question was not studied systematically.) The rest of the eyecup was stored in a moist light-tight box at 4 °C; viable pieces of retina could be obtained for at least 6 h after dissection. The retina of the second eye was isolated for visual inspection of the extent of the porphyropsin field, which could be clearly distinguished from the rhodopsin field by its violet colour.

Microspectrophotometry

Recording. A small piece of retina was placed in a drop of Ringer solution on a microscope slide and gently torn and shaken to produce isolated outer segments. The preparation was closed with a cover-slip and sealed at the edges with Vaseline. The microspectrophotometer, constructed in the Leningrad laboratory (Govardovskii & Zueva, 1988), was not equipped with an infra-red converter, so the field was examined and adjustments made using deep red light ($\lambda > 680$ nm). This light caused no significant bleaching for at least 10 min. The dimensions of the measuring beam varied from 2×35 to 3×45 μm. The light was linearly polarized in the plane of the discs of the outer segments.

Determination of pigment composition. The recorded spectra of ventral rods were accurately fitted with the Dawis (1981) nomogram for 502 nm rhodopsin (see Fig. 1*B* below). This agrees with earlier measurements on bull-frog rhodopsin in digitonin extracts, where λ_{max} has been determined with high accuracy (501·5 ± 1 nm; Reuter *et al.* 1971 and Tom Reuter, personal communication; see also Makino-Tasaki & Suzuki, 1984). Tsin & Beatty (1980) have reported $\lambda_{max} = 499$ nm, but presented no evidence that would make it possible to assess the significance of this deviation.

The dorsal rods were assumed to contain a mixture of $rhodopsin_{502}$ and a porphyropsin, for which λ_{max} could not, however, be inferred from our microspectrophotometry with accuracy better than *ca* ± 5 nm. We therefore had to rely on published evidence for the exact value to use when fitting

recorded spectra with sums of nomograms. There are two reasons for our choice of 523 nm rather than 522 nm as reported by Reuter *et al.* (1971) and Tsin & Beatty (1980). Firstly, the porphyropsin spectrum determined from a porphyropsin–rhodopsin mixture is liable to underestimate λ_{max} somewhat. Secondly, the difference between a rhodopsin at 502 nm and its corresponding porphyropsin would typically be larger than 20 nm (Bridges, 1967). It is worth emphasizing, though, that our conclusions would not be significantly affected by an error of one or two nanometres in the assumed porphyropsin absorbance peak.

Current recording from single rods

The techniques for suction pipette recording from single rods were basically as described by Baylor, Lamb & Yau (1979). Small pieces of retina (*ca* 0·5 mm square) were placed in a 300 μl Plexiglas chamber filled with Ringer solution. The recording pipette was introduced horizontally through the open side of the chamber, where the surface of the solution was continuously exposed to a stream of moist oxygen. A suitable rod protruding laterally from the piece of retina was selected under infra-red video inspection. The temperature in the chamber was between 17 and 19 °C and was measured with a microthermistor. The silanized pipettes had tip diameters of 7–8 μm and 'open' resistances of 2–3 MΩ. The resistances increased by 3- to 4-fold when a cell had been successfully drawn into the pipette, which was connected by an Ag–AgCl electrode to a current-to-voltage converter. The voltage signal was amplified (bandpass 0–4·3 Hz or 0·016–4·3 Hz, in some cases 0·016–10 Hz; 4-pole active Butterworth filter) and continuously recorded on an FM tape-recorder. In addition, light responses were recorded and stored on a digital averager. The records shown in the figures are penwriter tracings replayed from tape through the averager. During replay, long-lasting records were usually digitized at 100 ms intervals and then sent to the penwriter at a higher frequency (normally 40 ms per point), so the curves shown in the figures are somewhat low-pass filtered by the penwriter. Matched-filtered records (like those in Fig. 3) with effective bandwidth below 1 Hz are not affected by this procedure. When necessary, digitization was performed at a higher frequency.

Light stimulation

The light came from a stabilized source with interference filters and neutral density filters inserted in the beam. The transmittance of the filters was calibrated with a Hitachi 150–20 spectrophotometer. The light was plane-polarized with the electric vector approximately perpendicular to the axis of the rod. Stimuli were 50 ms full-field flashes delivered by an electromagnetic shutter. The unattenuated intensity of the light incident on the preparation (60 quanta $\mu m^{-2} s^{-1}$ at the stimulus wavelength 537 nm) was measured by a calibrated photomultiplier (calibration standards by the Institute of Metrology, Leningrad). Using estimated collecting areas, appropriate pigment densities (see Results) and a quantum efficiency of bleaching of 0·67, we obtained first estimates of the numbers of photoisomerizations that given light flashes were expected to produce in rods. This calibration, however, was used only to guide our initial choice of stimulus light intensities. In the quantitative analysis of the results we did not rely on this physical light calibration, but on statistical analysis of the recorded dark and light noise (see below).

The porphyropsin content of each cell intended for recording was characterized by its relative spectral sensitivity in the long-wavelength region, which could be quickly assessed as the ratio of sensitivities at 635 and 537 nm (S_{635}/S_{537}). The intensities of a 537 and a 635 nm stimulus were adjusted to elicit the same response amplitude, and the intensity ratio (I_{537}/I_{635}) was recorded. The mean ratio of the most short-wavelength-sensitive rods from the ventral retina was taken as 1. In porphyropsin-rich rods from the dorsal retina, this value, which will be referred to as the 'red/green ratio', varied between 4 and 6·1.

The specimen holder, manipulators, microscope and preamplifier were situated in a light-tight Faraday cage. During recordings, the light intensity in the cage as measured by the calibrated photomultiplier was less than one quantum per 500 s per rod. To exclude stray light even more rigorously, the specimen holder was further covered by a black box during the recordings.

Analysis

It was not possible to count discrete isomerization-like events reliably from the records, as the amplitude ratio of the discrete and continuous components (see Baylor *et al.* 1980) of the dark noise was not high enough. Attempts to improve the ratio by matched filtering (see Fig. 3) were not

particularly successful because of the similar spectral compositions of the two noise components. Therefore, the event rate was determined from frequency histograms of the dark current amplitude. The record was digitized at 10 or 20 Hz and the histogram of current values was plotted (cf. Fig. 4). Since the discrete events are unipolar current decrements, they add a small negative shoulder to an otherwise symmetrical noise amplitude distribution.

One way of estimating the event rate, f, from such a histogram (Baylor *et al.* 1980; Matthews, 1984) is by the first moment, M_1, which is equal to the mean value of the noise current, $\bar{\imath}$:

$$M_1 = \bar{\imath} = \int_{-\infty}^{\infty} i\,p(i)\,\mathrm{d}i = f\int_0^{\infty} i(t)\,\mathrm{d}t. \tag{1}$$

However, this requires that the zero level of the noise current (i.e. the mean value *without* discrete events) be known, which is not possible unless discrete events can be reliably sorted out by some independent method. Baylor *et al.* (1980) made the assumption that one tail of the distribution (the positive or right-hand tail in our Figs 4 and 6) was unaffected by discrete events and fitted it by a Gaussian presumed to represent the continuous component. This rationale, however, produces a systematic error, which in the conditions of our experiments was unacceptably large (up to 50% as found by computer simulation). Therefore, we chose to estimate both the frequency and the amplitude of discrete events by fitting the complete experimental histogram with the probability density function for the sum of Gaussian noise and randomly occurring events having the shape of the single-photon response. This function, $p(i)$ (the probability density for a given value i of the dark current), is obtained as the convolution integral of the probability densities for the discrete and the continuous components, p_d and p_c, assumed to be independent (Bendat & Piersol, 1966):

$$p(i) = \int_{-\infty}^{\infty} p_\mathrm{c}(i-x)\,p_\mathrm{d}(x)\,\mathrm{d}x, \tag{2}$$

where x is any current value that the discrete noise component may take on. (In our case, $p_\mathrm{d}(x) \neq 0$ only when $0 < x < x_\mathrm{max}$ (the amplitude of the quantal event), so the integral can be taken as the sum of two parts, from 0 to x_max and from x_max to 0.) p_c is a Gaussian of zero mean and variance σ^2 (the variance of the continuous noise).

To transform eqn (2) into a time integral, let the frequency of discrete events be f, and assume that the probability for two or more events to overlap is negligible ($1/f \gg$ the duration of a discrete event; analysis has shown that this does not significantly affect our results). Then the full record can be represented as a series of stretches of mean duration $1/f$, each containing one single discrete event, whereby $x = r(t)$ (the waveform of the discrete event) and $p_\mathrm{d}(x) = 1/|\mathrm{d}r/\mathrm{d}t|$ (normalizing factors omitted). Observing that $\mathrm{d}x = (\mathrm{d}r/\mathrm{d}t)\,\mathrm{d}t$, eqn (2) becomes

$$p(i) = \int_0^{1/f} \exp\left[-(i-r(t))^2/2\sigma^2\right]\mathrm{d}t. \tag{3}$$

Optimizing the fit of eqn (3) to the experimental histogram allows the determination of the interesting parameters with good accuracy. This is possible for the following reason. Although eqn (3) contains three parameters (*f.* σ and the single-quantum response amplitude), only two, (σ, f) *or* (σ, amplitude), can be varied freely to fit the histogram. The amplitude and the frequency of events are interconnected through the third moment M_3 (the skewness of the histogram), which can be calculated independently:

$$M_3 = \int_{-\infty}^{\infty} i^3 p(i)\,\mathrm{d}i = f\int_0^{\infty} r^3(t)\,\mathrm{d}t. \tag{4}$$

The use of eqn (4) rests on two assumptions: (1) the mean value of the recorded current is zero (AC recording); (2) the continuous noise is symmetrical, so the skewness is entirely due to discrete events. For the calculations of $p(i)$ and M_3, the waveform of the discrete event $r(t)$ was assumed to be indistinguishable from the single-quantum response. It was approximated by a four-stage 'Poisson' model response (Baylor, Hodgkin & Lamb, 1974; see eqn (5)) passed through the recording system, by which an excellent fit to recorded dim-flash responses could usually be obtained (Fig. 2*B*).

The goodness of fit of computed probability distributions and experimental histograms was judged by eye. In porphyropsin rods, the procedure generally allowed determination of the event

rate with an error of less than 10%, as assessed by computer simulations with a Gaussian noise generator.

The procedure also fixed the amplitude of the discrete event in porphyropsin rods with good precision. Changes of no more than ± 10% around an optimal value, with constant M_3, perceptibly degraded the fit of theoretical and experimental histograms (see Fig. 4, dotted lines). We therefore used the histogram analysis as our standard method for estimating the amplitude of discrete dark events in porphyropsin rods. On the other hand, we could independently determine the amplitude of the response to a single photoisomerization from the variance/mean ratio of the amplitudes in a sequence of responses to flashes of constant, very low mean intensity (see Baylor *et al.* 1979, 1980, 1984; Matthews, 1984). In each cell, the waveform of the averaged response from all flash presentations was used as a template for reading the amplitudes of the single responses. The amplitudes were measured manually from records plotted on expanded time scales as the change in current from the time around the flash to the time around the peak of the averaged response. In all our recordings from porphyropsin rods, the amplitude of the single-photon response thus determined agreed within ±20% with the dark event amplitude obtained from 'dark' histograms (see Table 1).

Estimation of effective light intensities. The amplitude of the discrete dark event as determined by histogram analysis in porphyropsin rods was also used for calculating the mean number of photoisomerizations per rod (denoted Rh*) per flash actually produced in each particular flash session. (The amplitude of the averaged flash response was divided by that of the discrete event.) By taking the grand mean of estimates from many cells (with due correction made for the volume of outer segment drawn into the pipette), the effect of quantal variation between single sessions could be eliminated, yielding a calibration which represents the estimate from an 'infinitely' long flash session. These intensity values are referred to as 'nominal intensities'. The nominal intensities for rhodopsin rods were obtained by correcting for the absorbance difference between rhodopsin and porphyropsin rods at the stimulus wavelength, 537 nm. All numbers and rates of light-induced isomerizations (Rh* or Rh* s^{-1}) given in the present work are based on this 'biological' calibration.

Rhodopsin rods. In rhodopsin rods, the dark current histogram was completely symmetrical (see Results), implying that discrete dark events were either very rare or very small, or both. Thus, neither the rate nor the amplitude could be directly estimated from the histogram alone. Instead, the single-quantum response amplitude was determined from flash sessions, and this amplitude was then used to estimate the possible rate of such events from the dark current histogram. The quantal amplitude was determined in two different ways: (1) by dividing the amplitude of the averaged flash response by the nominal flash intensity (as calibrated in experiments with porphyropsin rods); (2) by taking the ratio of response variance to mean response amplitude (see above). The estimates obtained by these two methods were in good agreement (see Table 1). In addition, some cells were exposed to dim steady illumination and their 'light' current histograms analysed (see Fig. 7).

RESULTS

Porphyropsin distribution in the bull-frog retina

Although our frogs were kept under conditions favouring a high proportion of porphyropsin (see Methods), there was considerable variation between animals in the size of the porphyropsin fields, as was evident even from a casual visual inspection of isolated retinas. In some cases, the porphyropsin was restricted to a narrow crescent in the dorsalmost part of the retina. To determine the pigment composition of different rods, we performed microspectrophotometric measurements on rod outer segments from various retinal locations.

The porphyropsin/rhodopsin ratio of the rods was determined by fitting the recorded spectra with sums of nomograms (Dawis, 1981) for rhodopsin$_{502}$ and porphyropsin$_{523}$ (see Methods). Thanks to the large dimensions of bull-frog rod outer segments, the quality of the absorption spectra was sufficient for a fairly accurate determination.

Figure 1 illustrates the fitting of nomograms to the spectra of a porphyropsin-rich

rod (Fig. 1*A*) and a rhodopsin rod (Fig. 1*B*). To fit the absorption spectrum in Fig. 1*A*. it was necessary to assume a 20% admixture of rhodopsin. It could not be satisfactorily fitted with any pure porphyropsin nomogram, regardless of λ_{max}. On the other hand, the spectrum in Fig. 1*B* contains no detectable trace of porphyropsin;

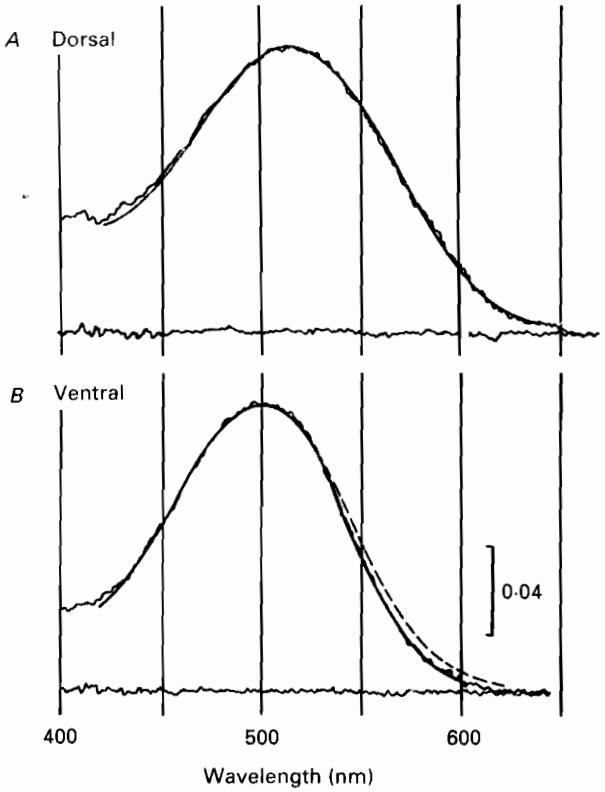

Fig. 1. Microspectrophotometric records of the absorption spectra of single rod outer segments from the dorsal (*A*) and ventral (*B*) retina. The spectrum of the dorsal rod is well fitted by the sum of nomogram curves for porphyropsin$_{523}$ and rhodopsin$_{502}$ in the molar ratio 0·8/0·2 (smooth curve in *A*). The ventral rod contained virtually pure rhodopsin (smooth continuous curve in *B*); a 10% admixture of porphyropsin could have been reliably detected (dashed curve in *B*). Vertical scale bar: absorbance.

the fit becomes perceptibly poorer if as small an admixture as 10% of porphyropsin$_{523}$ is assumed (dashed curve). We found that rods in the same restricted neighbourhood had quite similar pigment compositions which changed smoothly across the retina. This was ascertained by recording absorbance spectra in sequence from many rods protruding from the edges of relatively large (several millimetres) retinal pieces.

In rods from the dorsalmost part of the retina we found (molar) proportions of porphyropsin$_{523}$ ranging from 66 to 88% ($74 \pm 1{\cdot}3$%, $n = 38$). All rods from the ventral retina contained rhodopsin$_{502}$ without detectable contamination by porphyropsin. The validity of this conclusion depends, however, on the reliability of nomogram data in the long-wave end of the spectrum. Dawis' (1981) nomogram is based mainly on Dartnall's (1953) absorbance values for *Rana temporaria* rhodopsin,

but *R. catesbeiana* and *R. pipiens* rhodopsins in digitonin extracts show markedly lower absorbances beyond 580 nm than predicted by the Dartnall–Dawis nomogram (Tom Reuter, personal communication). The reason for this discrepancy is unclear, but if we adopt Reuter's values for the absorbance of bull-frog rhodopsin, our purest rhodopsin rods might contain 5% of porphyropsin.

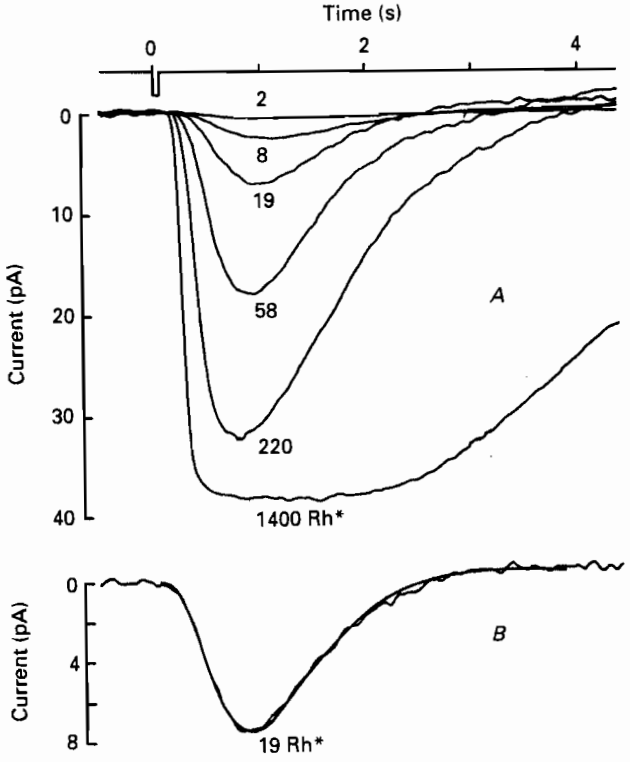

Fig. 2. *A*, family of superimposed responses from a ventral (rhodopsin) rod to 50 ms flashes of increasing intensity. The number of isomerizations (nominal intensity, see Methods) is shown beside the response in each case. The response to the dimmest flash is the average of sixteen trials; the larger responses are single sweeps. *B*, the response to nineteen isomerizations shown on expanded scales, fitted with a curve depicting the response of a four-stage 'Poisson' model with $\alpha = 3{\cdot}52\ s^{-1}$ (eqn (5) in the text) passed through the recording system. Bandwidth 0·016–10 Hz, digitization at 100 Hz. Temperature 19 °C.

As the pigment composition is the crucial factor in the present study, we regularly checked the absorption spectra of rods from the same small pieces of retina that were used for the electrophysiological experiments. The control pieces for the 'dorsal' cells listed in Table 1 contained $78{\cdot}9 \pm 1{\cdot}3$% of porphyropsin$_{523}$ ($n = 20$). In addition, the red/green ratio (see Methods) was determined in each porphyropsin rod intended for dark current recordings. The highest value of the ratio found was 6·1, which is assumed to correspond to the highest proportion of porphyropsin found by microspectrophotometry, 88%. For the dorsal rods listed in Table 1, the mean red/green ratio was $5{\cdot}5 \pm 0{\cdot}2$, which would indicate $77{\cdot}6 \pm 3{\cdot}5$% of porphyropsin.

Surprisingly, there was no significant difference in specific absorbance between rhodopsin and porphyropsin rods ($0{\cdot}0156 \pm 0{\cdot}002\ \mu m^{-1}$ and $0{\cdot}0146 \pm 0{\cdot}005\ \mu m^{-1}$, respectively). The mean dichroic ratio was 3 in both cell types. Assuming the molar absorbance of rhodopsin to be $40600\ cm^{-1}\ M^{-1}$ and that of porphyropsin to be

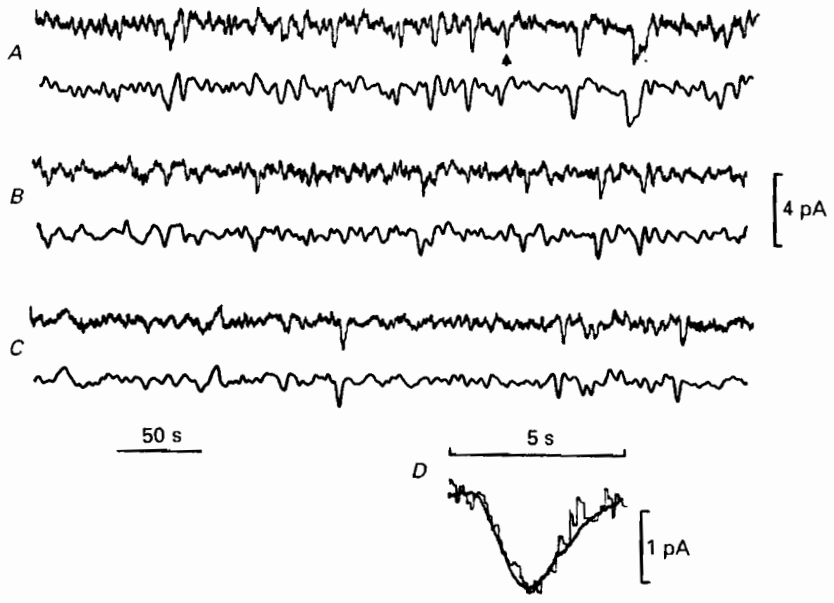

Fig. 3. The outer segment current of a porphyropsin rod in darkness (cell No. 5 in Table 1). Each pair of traces (*A*, *B* and *C*) represents one uninterrupted 400 s dark recording; in each pair, the lower (smoother) record is a matched-filtered version of the upper one. Between two subsequent dark sessions, the sensitivity of the cell (response amplitude per isomerization) was monitored by recording a sequence of dim-flash photoresponses (not shown). In *D*, the waveform of one 'discrete' negative deflection (indicated by an arrow in *A*) is compared with the averaged photoresponse to the mean flash intensity 2·2 Rh* (sixteen presentations). The amplitude of the averaged response has been reduced by the factor 2·2 and is then seen to give a good fit to the event. The saturating response amplitude of this cell was 33 pA. The red/green ratio was 5·8, corresponding to 83% porphyropsin. Recording bandwidth 0·016–4·3 Hz, digitization at 10 Hz for the long recordings and at 100 Hz for the averaged response. The left-hand time calibration bar (50 s) refers to the long records (*A–C*); the right-hand bar (5 s) to record *D*. Temperature 17 °C.

$30000\ cm^{-1}\ M^{-1}$ (Dartnall, 1972), we obtain visual pigment concentrations of 3 mM for (pure) rhodopsin, and 2·7 mM for the porphyropsin in a 0·8/0·2 porphyropsin/rhodopsin mixture (per litre total outer segment volume). These values were used for the calculation of the numbers of visual pigment molecules per rod outer segment.

General response properties

The basic response properties were similar in rhodopsin and porphyropsin rods. A family of responses from a rhodopsin rod to flashes of different intensities is shown in Fig. 2*A*. The waveforms and intensity dependence are similar to those observed

in current responses from toad rods (Baylor *et al.* 1979, 1980; Lamb, 1984). The amplitude of saturated responses varied between 8 and 55 pA, and the half-saturating flash intensity was approximately 20 Rh* in sensitive cells. The amplitude of the single-quantum response was 0·4–3·5 pA. Dim-flash responses could usually be

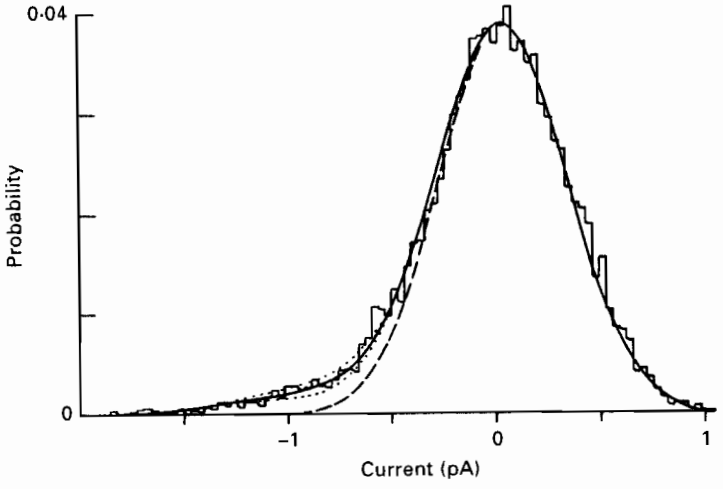

Fig. 4. Dark current amplitude histogram for the porphyropsin rod in Fig. 3, with superposed theoretical probability distributions (smooth curves). Abscissa: outer segment current amplitude relative to mean level; inward current positive. The dashed curve is a Gaussian of standard deviation 0·32 pA, representing the continuous noise component. The continuous line is the theoretical current distribution for the sum of the single-photon response and the continuous noise, calculated according to eqn (3) in the text, with the amplitude of the discrete event 1·2 pA and the rate of events 0·024 s^{-1}. The dotted lines have been computed for event amplitudes 10% larger and smaller than the optimal 1·2 pA, i.e. 1·32 and 1·09 pA (M_3 = constant then gives event rates 0·018 and 0·032 s^{-1}, respectively). They are shown to demonstrate how sensitive the analysis is to the amplitude of the discrete event. Recording bandwidth 0·016–4·3 Hz, digitization at 10 Hz. Record duration 1178 s, histogram bin width 0·032 pA.

well described by a four-stage 'Poisson' model (Fuortes & Hodgkin. 1964; Baylor *et al.* 1974, 1979), as illustrated in Fig. 2*B*:

$$r(t) = kI(\alpha t)^3 e^{-\alpha t}, \tag{5}$$

where I is the flash photon density, k is a sensitivity constant and α is a rate constant.

Dark noise in porphyropsin rods

Experimental protocol

Both porphyropsin and rhodopsin rods were subjected to the same experimental protocol. When the rod had been successfully drawn into the pipette, the saturated response amplitude, sensitivity, and red/green ratio were determined. After that, 160 s 'light' sessions alternated with 400 s 'dark' sessions. During a light session, the cell was stimulated at 10 s intervals with dim (*ca* 1·5 Rh*) 537 nm flashes. Thus, the

sensitivity of the cell (pA/Rh*) was monitored. The dark noise was estimated from dark records obtained between successive light sessions.

Discrete events

Figure 3 displays three dark recordings from a porphyropsin rod. Superposed on a more or less symmetrical 'continuous' noise, 'discrete' negative deflections resembling single-photon responses can be distinguished. To illustrate the similarity, the deflection marked by an arrow in *A* is plotted together with the averaged single-photon response on expanded scales in panel *D*. In the top trace of Fig. 3, it is possible to count at least eight such putative discrete events. Such deflections could readily be seen in all porphyropsin rods where the recording was silent enough. However, it was often impossible to decide whether a deflection represented a discrete event distorted by noise, or just an unusually large excursion of the continuous noise. Matched filtering did not improve the situation much, as seen from the lower records (smoother traces) in each of the pairs *A*, *B* and *C* in Fig. 3. Hence, the frequency of discrete dark events could not be reliably estimated by direct counting.

Our quantitative estimates were therefore always based on analysis of the frequency histogram of the dark current amplitude, as shown in Fig. 4. A detailed description of the analysis is given in the Methods section. The mean frequency of discrete events thus estimated from the dark current of six porphyropsin rods at 18 °C was 0·027 s^{-1} (Table 1). The outer segment volumes given in Table 1 (mean 1875 μm^3) refer to the part apparently inside the pipette, measured from the tip of the pipette. Since the constriction separating 'inside' from 'outside' does not in fact lie at the tip, it was (somewhat arbitrarily) assumed that the recordings were made from approximately 75% of that volume; this gives a mean recording volume of 1400 μm^3. Recalculated to the whole volume of an average bull-frog rod (3000 μm^3), the event frequency then becomes 0·057 rod^{-1} s^{-1}.

Continuous noise

The Gaussian or continuous component of the recorded dark current noise (see Fig. 4) also appeared to be mainly of cellular origin. The variance of the instrumental noise recorded with an open pipette was normally just above the Johnson noise level expected from the resistance of the pipette, and in matched-filtered records (reducing the effective bandwidth to *ca* 0·5 Hz), the open-pipette noise was negligible compared with the fluctuations of the current when a rod had been sucked in. The standard deviation σ of the continuous noise stood in a fairly constant ratio ($0{\cdot}32 \pm 0{\cdot}02$, $n = 11$) to the amplitude of the quantal response, despite substantial variation in the absolute values recorded from different cells. This was true of both porphyropsin and rhodopsin rods. The Pearson coefficient for linear correlation between σ and the single-photon response amplitude for the cells in Table 1 is $r = 0{\cdot}96$. This correlation is hardly due to the trivial possibility that the pipette records varying proportions of the outer segment current, because in the same sample of cells the amplitudes of the quantal response and the saturated response correlated but weakly ($r = 0{\cdot}47$). Whatever the reason for the variation in absolute values, the strong correlation suggests that the continuous noise largely stems from the same

source as the discrete events, i.e. the phototransduction machinery of the rod (cf. Baylor *et al.* 1980).

Dark noise in rhodopsin rods

When stimulated with flashes of light, rhodopsin and porphyropsin rods behaved very similarly. The single-photon response amplitudes were similar (see Table 1), and

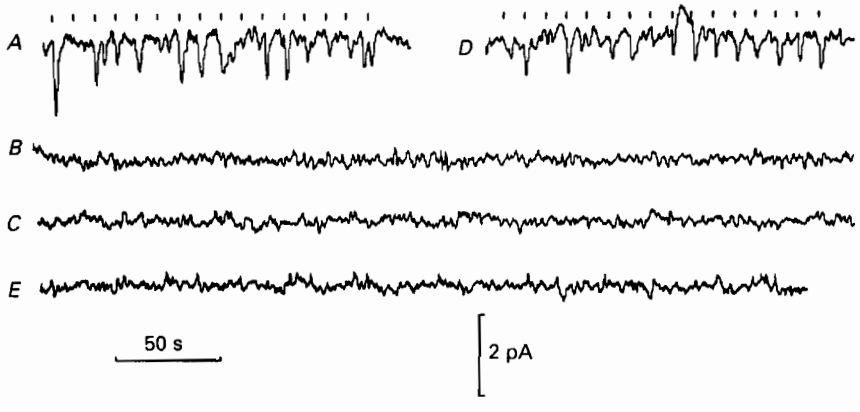

Fig. 5. Outer segment current of a rhodopsin rod (No. 9 in Table 1) in darkness (*B*, *C* and *E*) and when presented with dim flashes at 10 s intervals (*A* and *D*). The alphabetical order *A* to *E* corresponds to the sequence of recording. The saturating response amplitude was 8·2 pA. The single-quantum response amplitude as determined by relying on the nominal flash intensity (1·25 Rh*) was 0·43 pA; as determined from the variance-to-mean ratio of thirty-two flash responses it was 0·39 pA. The standard deviation of the continuous noise was 0·13 pA. No clear discrete events are seen during the dark records (comprising 1188 s). Temperature 17 °C.

in both cell types repeated stimulation with flashes of constant low mean intensity elicited response amplitudes which varied in a manner suggestive of Poisson variation in the numbers of isomerizations produced on each presentation (cf. Fig. 5*A* and *D*).

To our surprise, however, it was usually impossible to detect any convincing discrete events in the dark records of rhodopsin rods. In Fig. 5*B*, *C* and *E*, not one single such event can be identified during 20 min of dark recording. Consistent with that, the dark current amplitude histogram displayed in Fig. 6 appears completely symmetrical, with no hint of the occurrence of unipolar events. As shown by the negative tail of the distribution displayed on expanded scales in Fig. 6*B*, the upper limit to a discrete event rate that might pass undetected lies at *ca* 0·005 Rh* s^{-1}.

It might be argued that the apparent absence of discrete events is due only to our inability to detect them. If, for instance, the light calibration were slightly inaccurate and the cells showed some kind of 'supralinear' behaviour (Capovilla, Cervetto & Torre, 1983), responses to single photoisomerizations might be submerged in the continuous noise and those which we interpret as single-quantum responses could in fact be due to two or more isomerizations. We tested this possibility by recording the current of rhodopsin rods during illumination with steady background lights of nominal intensity less than 0·1 Rh* s^{-1}. In these conditions, the probability of

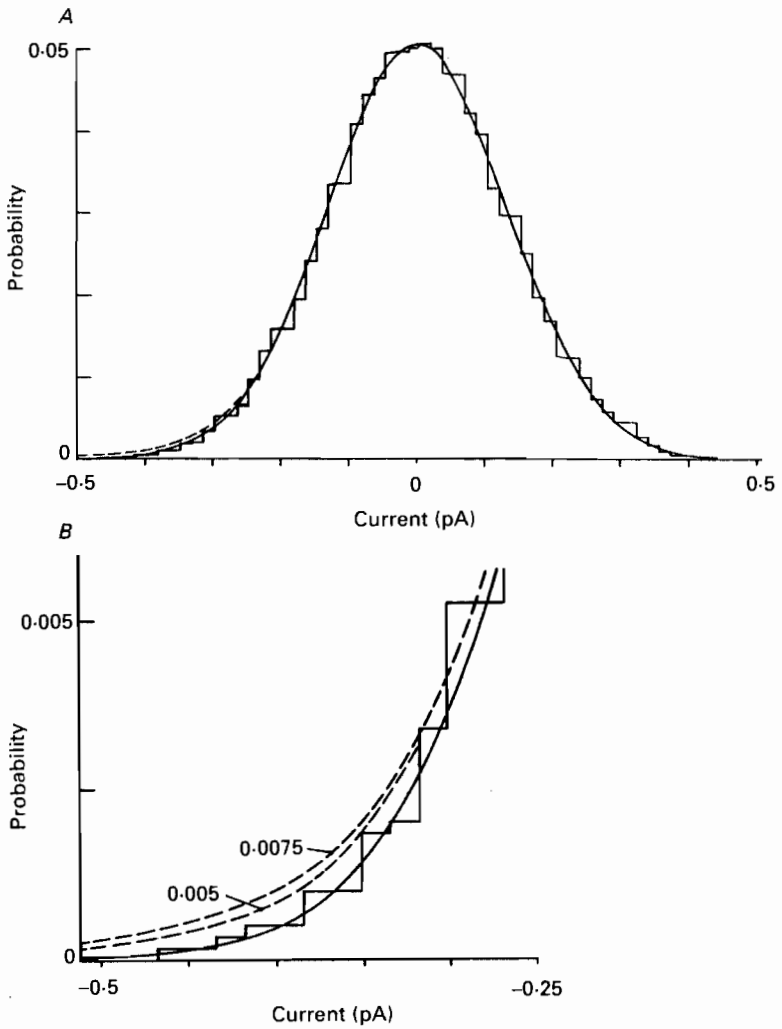

Fig. 6. *A*, dark current amplitude histogram and theoretical probability distributions for the rhodopsin rod in Fig. 5. 1230 s dark record digitized at 20 Hz. Recording bandwidth 0·016–4·3 Hz; histogram bin width 0·016 pA. The continuous curve is a Gaussian of unit area and standard deviation 0·13 pA. The dashed curve gives the probability distribution according to eqn (3) under the assumption that discrete isomerization-like events of 0·43-pA amplitude occur at a rate of 0·0075 s^{-1}. *B*, the negative tail of the histogram in *A* on expanded scales. The dashed curves give the probability densities for dark event rates 0·0075 and 0·005 s^{-1}. The latter value approximately represents the lowest rate that would be detected by our analysis.

coincidence of two quanta is low, and if a substantial number of discrete events are observed, most of them must be responses to single isomerizations. In these experiments, the isomerization rates and single-quantum response amplitudes could be estimated from the amplitude histogram of rod current under background illumination.

Figure 7 shows the results of one such experiment, with a nominal steady intensity of 1 Rh* per 11·3 s, and including also a sequence of responses to 0·9 Rh* flashes in darkness (trace *A*). Events similar to the flash responses in *A* are readily seen in the presence of the background (trace *B*), but not in darkness (trace *C*). The analysis of

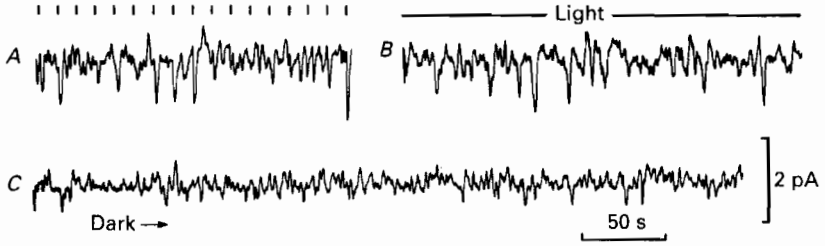

Fig. 7. Light and dark noise in a rhodopsin rod (cell No. 8 in Table 1). *A*, responses to 0·9 Rh* flashes. *B*, photon noise during continuous illumination of nominal intensity 1 Rh* per 11·3 s. An analysis of the current amplitude histogram (such as shown in Figs 4 and 6) indicated one isomerization event per 12·5 s and event amplitude 0·77 pA. The single-quantum response amplitude as estimated from the variance-to-mean ratio of the responses to thirty-two flashes was 0·88 pA. *C*, 404 s dark record. The frequency of discrete dark events was below the resolution limit 0·005 s^{-1} (1 Rh* per 200 s) of the dark current amplitude histogram analysis. The saturating response amplitude was 29·4 pA; the standard deviation of the continuous noise was 0·22 pA. Temperature 17·5 °C.

the current amplitude histogram indicated a mean event rate of one per 12·5 s during background, close to the nominal intensity of the background, and event amplitude 0·77 pA. The amplitude of the single-quantum response as determined from the variance-to-mean ratio of thirty-two flash responses was 0·88 pA. We used the more cautious value (0·77 pA) to estimate the rate of possible dark events from the dark current histogram, arriving at an upper limit of one event per 200 s.

It is worth noting that the negative deflections of the dark current (i.e. in the direction of photoresponses) in Fig. 7*C* correspond fairly closely to what is expected solely from Gaussian noise with zero mean and the variance of the continuous component. Inspecting a matched-filtered version of the dark record, we found that five negative peaks, encompassing twenty-eight of all the 4040 points in the digitized record (i.e. the fraction 0·0069), reach beneath the current level defined by $-2{\cdot}5\sigma$ where σ is the standard deviation of the matched-filtered continuous noise. This is close to the probability 0·0062 for a stochastic normally distributed variable to fall below $-2{\cdot}5\sigma$. Moreover, the dark current never reaches down to the -3σ level, still less to the level corresponding to the single-quantum response amplitude ($-3{\cdot}7\sigma$ in the matched-filtered record).

It is more difficult to judge the probability of obtaining 'false negatives' when records are visually examined, i.e. the probability for an isomerization-like event not to reach a detection criterion because of superposition on the continuous noise and intrinsic variability of the event amplitude. If the continuous noise is the only source of variability, the probability that an event of amplitude $3{\cdot}7\sigma$ shall fail to cross the 3σ level is 0·24, that for two events 0·06 and that for three events 0·014. If it is assumed that event amplitudes have a total standard deviation twice that of the

TABLE 1. Dark noise in porphyropsin and rhodopsin rods of the bull-frog retina

Cell	Temperature (°C)	Record duration (s)	Saturated response amplitude (pA)	Amplitude of quantal event: Dark event (pA)	Amplitude of quantal event: Single-photon response: Method I (pA)	Amplitude of quantal event: Single-photon response: Method II (pA)	Standard deviation of continuous noise (pA)	Frequency of discrete events (s^{-1})	Sucked rod outer segment volume (μm^3)	Activation rate constant ($\times 10^{-11}$ s^{-1})
					Dorsal retina (porphyropsin)					
1	18·5	1230	16	0·74		0·72 (64)	0·22	0·035	2160	1·33
2	19·5	1230	12·7	0·44		0·50 (32)	0·21	0·025	1910	1·08
3	17	1219	24·8	0·83		0·94 (32)	0·26	0·046	2100	1·80
4	17	820	18·8	0·69		0·76 (16)	0·22	0·014	1760	0·65
5	17	1178	33	1·20		1·08 (37)	0·32	0·024	1550	1·27
6	18	1229	13·5	1·42		1·20 (32)	0·40	0·019	1770	0·88
					Ventral retina (rhodopsin)					
7	19	1628	12·5		0·62	0·46 (32)	0·20	0·006	3030	0·15
8	17·5	819	29·4		0·77	0·88 (32)	0·22	< 0·005	3000	Not determined
9	17	1230	8·2		0·43	0·39 (32)	0·13	< 0·005	1190	Not determined
10	19	819	9·8		0·45	0·49 (32)	0·13	< 0·005	960	Not determined
11	17	819	13·2		0·40	0·46 (32)	0·13	< 0·005	2510	Not determined

The single-quantum response amplitudes given under 'Method I' were determined by dividing the mean amplitude of a series of dim-flash responses by the nominal flash intensity (Rh*). Those given under 'Method II' were obtained as the ratio of response variance to mean response amplitude: the number in parentheses gives the number of flash responses underlying the determination in each case. The amplitudes of dark events in porphyropsin rods were determined from the dark current amplitude histograms as described in the text.

In seven other rhodopsin rods (not included in the table), three putative discrete events were detected by visual inspection of totally 3620 s recordings, suggesting the activation rate constant $0{\cdot}023 \times 10^{-11}$ s^{-1} for rhodopsin. The photopigment activation rate constants were computed assuming that the mean concentration of porphyropsin in the rods was 2·7 mM, that of rhodopsin 3 mM, and that the recordings were made from approximately 75% of the outer segment volume seemingly inside the pipette. A possible contribution of the *ca* 20% rhodopsin to the dark noise of porphyropsin rods was neglected. The mean of the activation rate constants for porphyropsin in the table, weighted by the durations of the records from which they were determined, is $1{\cdot}2 \pm 0{\cdot}2 (\times 10^{-11}$ $s^{-1})$.

dark current (see Baylor *et al.* 1984), the corresponding probabilities would be 0·36, 0·13 and 0·05. Then, for example, if records that in fact contain two discrete events each are scanned with a 3σ criterion, in one case out of seven both events would be missed. It will be noted that the resolution limit of the histogram analysis (0·005 s^{-1}, see Table 1) leaves the possibility that, on average, every dark session (400 s) may contain two undetected events. These considerations give some confidence in estimation by visual inspection, the only method used by us in seven rhodopsin rods where less-complete records were obtained (see legend to Table 1).

It thus appears unlikely that the rarity of discrete events in rhodopsin rods is an experimental artifact. Table 1 summarizes the important response and noise parameters for the six porphyropsin rods and five rhodopsin rods where at least two dark sessions were successfully completed.

DISCUSSION

Do discrete events reflect thermal isomerization of the visual pigment?

The idea that the discrete dark events are due to thermal isomerization of the photopigment has been challenged on the basis of evidence from the compound eye (Barlow, 1989). In *Limulus*, the frequency of 'quantum bumps' can be influenced by e.g. diurnal rhythm and efferent innervation (Barlow, Kaplan, Renninger & Saito, 1987), which is difficult to reconcile with a thermal process. According to present knowledge of transduction in vertebrate rods, an event having the same shape as a single-photon response must be initiated in the visual pigment molecule itself, before the first stage of amplification. It would seem natural to identify this thermal initiation as an isomerization of the chromophore, which is the event that normally triggers the phototransduction cascade. The thermal parameters of the relevant noise component in dogfish bipolar cells (Ashmore & Falk, 1977, 1982) and toad rods (Baylor *et al.* 1980) are consistent with this idea. Our results showing that the rate of rod dark events depends on the chromophoric group in otherwise apparently identical pigments provide some additional support. In the absence of a conclusive identification, however, we shall cautiously refer to the initiating event only as an activation of the pigment molecule.

In Table 1, rate constants for the thermal activation of bull-frog porphyropsin and rhodopsin have been calculated from the frequencies of discrete events by use of the measured densities of the pigments in rods.

The probability of thermal activation bears no simple relation to the absorption spectrum

The rate constant for thermal activation of bull-frog porphyropsin obtained here (taken as the mean of the values in Table 1, weighted by the durations of the records from which they were derived) is $1{\cdot}2 \times 10^{-11}$ s^{-1}. This is less than 60 % higher than the value reported for toad rhodopsin, $0{\cdot}77 \times 10^{-11}$ s^{-1} at 18 °C (Baylor *et al.* 1980). The difference is certainly far smaller than the more than 50-fold difference predicted from a simple consideration of the energy barriers for photoexcitation of the two pigments (Barlow, 1957). Moreover, bull-frog rhodopsin, which has the same wavelength of peak absorption as toad rhodopsin (Hárosi, 1975), was found to be at least 5 times more stable (Table 1). Both these discrepancies indicate that the

molecular changes triggered by light and by thermal energy, respectively, proceed by different routes. There seems to exist no necessary physico-chemical relation between the absorption peak and the probability of thermal activation of a pigment. (This does not, of course, exclude the possibility that some more subtle feature of the absorption spectrum could carry information about thermal stability. Also, the possibility of spectral (Bowmaker, Loew & Liebman, 1975) and/or chemical (Bowmaker & Loew, 1976) polymorphism of frog rhodopsin appears intriguing in this light.)

It is worth noting that the toad and bull-frog rates of spontaneous rhodopsin activation may well differ by much more than the factor 5. Firstly, that factor is limited by the resolution of our analysis. Secondly, we cannot exclude that some discrete events in rhodopsin rods could be due to a small admixture of porphyropsin. In fact, we cannot estimate any meaningful *lower* limit for the rate of discrete events in bull-frog rhodopsin rods.

General correlation between absorption spectra and thermal stability

Available data still suggest that a red shift in the absorption maximum is in general accompanied by lower thermal stability. Rate constants for thermal activation have been determined for three porphyropsins: bull-frog (present study: $\lambda_{max} = 523$ nm, rate constant $1{\cdot}2 \times 10^{-11}$ s^{-1}), the hybrid sturgeon *Huso huso* × *Acipenser nudiventris* ($\lambda_{max} = 538$, rate constant 7×10^{-11} s^{-1}) and the sturgeon *Acipenser baeri* ($\lambda_{max} = 549$ nm, rate constant $1{\cdot}06 \times 10^{-10}$ s^{-1}) (Firsov & Govardovskii, 1990). In this admittedly limited material, there is a monotonic increase of the thermal activation rate with λ_{max}. This tendency could be important in the selection of visual pigments for a given mode of life in a particular light environment.

It must be emphasized, however, that the bull-frog's use of porphyropsin rather than rhodopsin for underwater vision cannot be understood in terms of the signal/noise ratio attained at the *absolute* threshold. Even in a 'favourable' case (deep in yellow fresh water with maximal transmission at 590 nm: see Jerlov, 1968), porphyropsin$_{523}$ will absorb at most 3 times more light than rhodopsin$_{502}$. Meanwhile, the frequency of isomerization-like events due to the porphyropsin is more than 8 times higher. Thus, the noise standard deviation will also be larger by at least 3-fold, and performance at the absolute threshold will not improve. Rather, the higher capacity of porphyropsin to catch photons in fresh water could become a dominant advantage in suprathreshold visual tasks, where the statistical fluctuations in the number of quanta is the main source of noise. Another possibility is that the ecological significance has to do with cone rather than rod vision. The distribution of retinal$_1$ and retinal$_2$ in the retina determines the character not only of the pigments in red rods, but of those in cones and green rods as well (cones: Semple-Rowland & Goldstein, 1981; green rods: Makino-Tasaka & Suzuki, 1984).

Are opsins that have to co-operate with retinal$_2$ particularly stabilizing?

The present data show that both the chromophore and the protein can influence the thermal stability of the pigment. Further experiments are needed to clarify the relative roles of these factors. It may be hypothesized that the structure of bull-frog opsin has been selected to compensate for the intrinsic instability of the long-

wavelength 3-dehydroretinal chromophore. Then the low noise in bull-frog rhodopsin rods compared with those of the toad could be a consequence of combining this highly stabilizing opsin with the relatively stable retinal$_1$ chromophore. Interestingly, no *Bufo* species hitherto studied (including *Bufo marinus*) has been found to use porphyropsin even in the tadpole stage (Peskin, 1957; Crescitelli, 1958; Muntz & Reuter, 1966), whereas all *Rana* tadpoles investigated have a large proportion of porphyropsin (Wilt, 1959; Muntz & Reuter, 1966). In other words, it seems that toad opsin, in contrast to frog opsin, never needs to co-operate with the retinal$_2$ chromophore. Whether this correlates with a consistent difference between the opsins of toads and frogs is a question that would merit further study.

Discrete rod events and the dark light

The insight that the thermal stability of a visual pigment is in no simple way determined by the spectral absorption characteristics, but subject to independent natural selection, has important consequences. The hypothesis that the absolute sensitivity is limited by noise from 'dark' isomerizations draws much of its fundamental beauty from the idea that non-negligible thermal activation is an inescapable property of the excitable molecules used for vision (Autrum, 1943; Stiles, 1948; de Vries, 1948; Barlow, 1957; Donner, 1989). This would set an irreducible noise level, while, on that view, many other noise sources could be reduced by natural selection. The apparent stability of bull-frog rhodopsin casts serious doubt on this idea. It makes the similarity in temperature-corrected dark event rates of rhodopsin rods in toad and monkey (Baylor *et al.* 1980, 1984) as well as dogfish (Ashmore & Falk, 1977, 1982) appear as either fortuitous, or as the result of evolutionary convergence. A third possibility is that the highly stabilizing bull-frog opsin is indeed a unique evolutionary innovation. It also forces a re-evaluation of correlations between the dark light measured in one species and rod event rates recorded in other species (Baylor *et al.* 1984; Donner, Hydén & Reuter, 1986; Reuter, Donner & Copenhagen, 1986; Aho, Donner, Hydén, Reuter & Orlov, 1987; Aho *et al.* 1988; Donner, 1989).

Note added in proof. A recent work by Corson, Cornwall, MacNichol, Mani & Crouch (1990) shows that incorporation of 4-hydroxyretinal as chromophore in the pigment of *Ambystoma tigrinum* rods induces excess membrane fluctuations with a power spectrum similar to that of the photon response. The apparent instability of the artificial pigment indicates the importance of the chromophore as such; the spectral shift in this case is towards the blue compared with native rhodopsin (λ_{max} = 470 nm and 520 nm, respectively).

We are much indebted to Professor Tom Reuter for his valuable suggestions and stimulating discussions. We are also grateful for the statistical advice of Dr Mikhail V. Vorobyev. This work formed part of joint project No. 22 of the Academy of Sciences of the USSR and the Academy of Finland. K. D. was also supported by grant 01/455 of the Academy of Finland.

REFERENCES

AHO, A.-C., DONNER, K., HYDÉN, C., LARSEN, L. O. & REUTER, T. (1988). Low retinal noise in animals with low body temperature allows high visual sensitivity. *Nature* **334**, 348–350.
AHO, A.-C., DONNER, K., HYDÉN, C., REUTER, T. & ORLOV, O. YU. (1987). Retinal noise, the

performance of retinal ganglion cells, and visual sensitivity in the dark-adapted frog. *Journal of the Optical Society of America A* **4**, 2321–2329.

ASHMORE, J. F. & FALK, G. (1977). Dark noise in retinal bipolar cells and stability of rhodopsin in rods. *Nature* **270**, 69–71.

ASHMORE, J. F. & FALK, G. (1982). An analysis of voltage noise in rod bipolar cells of the dogfish retina. *Journal of Physiology* **332**, 273–297.

AUTRUM, H. (1943). Uber kleinste Reize bei Sinnesorganen. *Biologisches Zentralblatt* **63**, 209–236.

BARLOW, H. B. (1956). Retinal noise and absolute threshold. *Journal of the Optical Society of America* **46**, 634–639.

BARLOW, H. B. (1957). Purkinje shift and retinal noise. *Nature* **179**, 255–256.

BARLOW, R. B. JR (1989). Is photoreceptor noise caused by thermal isomerization of rhodopsin? *Investigative Ophthalmology and Visual Science*, suppl. 30, 61.

BARLOW, R. B. JR, KAPLAN, E., RENNINGER, G. H. & SAITO, T. (1987). Circadian rhythms in *Limulus* photoreceptors. I. Intracellular studies. *Journal of General Physiology* **89**, 353–378.

BAYLOR, D. A., HODGKIN, A. L. & LAMB, T. D. (1974). The electrical response of turtle cones to flashes and steps of light. *Journal of Physiology* **242**, 685–727.

BAYLOR, D. A., LAMB, T. D. & YAU, K.-W. (1979). The membrane current of single rod outer segments. *Journal of Physiology* **288**, 589–611.

BAYLOR D. A., MATTHEWS, G. & YAU, K.-W. (1980). Two components of electrical dark noise in toad retinal rod outer segments. *Journal of Physiology* **309**, 591–621.

BAYLOR, D. A., NUNN, B. J. & SCHNAPF, J. L. (1984). The photocurrent, noise and spectral sensitivity of rods of the monkey *Macaca fascicularis*. *Journal of Physiology* **357**, 575–607.

BENDAT, J. S. & PIERSOL, A. G. (1966). *Measurement and Analysis of Random Data*. Wiley, New York.

BOWMAKER, J. K. & LOEW, E. R. (1976). The action of hydroxylamine on visual pigments in the intact retina of the frog (*Rana temporaria*). *Vision Research* **16**, 811–818.

BOWMAKER, J. K., LOEW, E. R. & LIEBMAN, P. A. (1975). Variation in the λ_{max} of rhodopsin from individual frogs. *Vision Research* **15**, 997–1003.

BRIDGES, C. D. B. (1967). Spectroscopic properties of porphyropsins. *Vision Research* **7**, 349–369.

CAPOVILLA, M., CERVETTO, L. & TORRE, V. (1983). The effect of phosphodiesterase inhibitors on the electrical activity of toad rods. *Journal of Physiology* **343**, 277–294.

COPENHAGEN, D. R., DONNER, K. & REUTER, T. (1987). Ganglion cell performance at absolute threshold in toad retina: effects of dark events in rods. *Journal of Physiology* **393**, 667–680.

CORSON, D. W., CORNWALL, M. C., MACNICHOL, E. F., MANI, V. & CROUCH, R. K. (1990). Transduction noise induced by 4-hydroxy retinals in rod photoreceptors. *Biophysical Journal* **57**, 109–115.

CRESCITELLI, F. (1958). The natural history of visual pigments. *Annals of the New York Academy of Sciences* **74**, 230–255.

DE VRIES, H. (1948). Der Einfluss der Temperatur des Auges auf die spektrale Empfindlichkeitskurve. *Experientia* **4**, 357–358.

DARTNALL, H. J. A. (1953). The interpretation of spectral sensitivity curves. *British Medical Bulletin* **9**, 24–30.

DARTNALL, H. J. A. (1972). Photosensitivity. In *Handbook of Sensory Physiology*, vol. VII/1, ed. DARTNALL, H. J. A. Springer, Berlin.

DAWIS, S. M. (1981). Polynomial expression of pigment nomograms. *Vision Research* **21**, 1427–1430.

DONNER, K. (1989). The absolute sensitivity of vision: can a frog become a perfect detector of light-induced and "dark" rod events? *Physica scripta* **39**, 133–140.

DONNER, K., HYDÉN, C. & REUTER, T. (1986). Noise and absolute threshold of frog retinal ganglion cells. *Acta universitatis Ouluensis A* **179**, 35–39.

FIRSOV, M. L. & GOVARDOVSKII, V. I. (1990). Dark noise of visual pigments with different absorption maxima. *Sensornye Sistemy* **4**, 25–34 (in Russian).

FUORTES, M. G. F. & HODGKIN, A. L. (1964). Changes in time scale and sensitivity in the ommatidia of *Limulus*. *Journal of Physiology* **172**, 239–263.

GOVARDOVSKII, V. I. & ZUEVA, L. V. (1988). A simple, high-sensitive recording microspectrophotometer. *Tsitologiya* **30**, 499–502 (in Russian).

HÁROSI, F. I. (1975). Absorption spectra and linear dichroism of some amphibian photoreceptors. *Journal of General Physiology* **66**, 357–382.

JERLOV, N. G. (1968). *Optical Oceanography*. Elsevier, London.

LAMB, T. D. (1984). Effects of temperature changes on toad rod photocurrents. *Journal of Physiology* **346**, 557–578.

MAKINO, M., KUZUO, N. & SUZUKI, T. (1983). Seasonal variation of the vitamine A_2-based visual pigment in the retina of the adult bullfrog, *Rana catesbeiana*. *Vision Research* **23**, 199–204.

MAKINO-TASAKA, M. & SUZUKI, T. (1984). The green rod pigment of the bullfrog, *Rana catesbeiana*. *Vision Research* **24**, 309–322.

MATTHEWS, G. (1984). Dark noise in the outer segment membrane current of green rod photoreceptors from toad retina. *Journal of Physiology* **349**, 607–618.

MUNTZ, W. R. A. & REUTER, T. (1966). Visual pigments and spectral sensitivity in *Rana temporaria* and other European tadpoles. *Vision Research* **6**, 601–618.

PESKIN, J. C. (1957). The visual pigments of amphibians. *Anatomical Record* **128**, 600.

REUTER, T., DONNER, K. & COPENHAGEN, D. R. (1986). Does the random distribution of discrete photoreceptor events limit the sensitivity of the retina? *Neuroscience Research*, suppl. 4, S163–180.

REUTER, T. E., WHITE, R. H. & WALD, G. (1971). Rhodopsin and porphyropsin fields in the adult bullfrog retina. *Journal of General Physiology* **58**, 351–371.

SEMPLE-ROWLAND, S. L. & GOLDSTEIN, B. E. (1981). Segregation of vitamin A_1 and vitamin A_2 cone pigments in the bullfrog retina. *Vision Research* **21**, 825–828.

STILES, W. S. (1948). The physical interpretation of the spectral sensitivity curve of the eye. In *Transactions of the Optical Convention of the Worshipful Company of Spectacle Makers*, pp. 97–107. Spectacle Makers' Co., London.

TSIN, A. T. C. & BEATTY, D. D. (1980). Visual pigments and vitamins A in the adult bullfrog. *Experimental Eye Research* **30**, 143–153.

WILT, F. H. (1959). The differentiation of visual pigments in metamorphosing larvae of *Rana catesbeiana*. *Developmental Biology* **1**, 199–233.